Silicon (2023) 15:2067–2082
https://doi.org/10.1007/s12633-022-02160-1

ORIGINAL PAPER

Synthesis and Solution Properties Evaluation of AATA Quaternary Copolymer

Tianhong Zhao[1,2] · Qiongqiong Guo[1,2] · Sijia Li[1,2] · Wushan Sun[1,2]

Received: 4 July 2022 / Accepted: 3 October 2022 / Published online: 13 October 2022

Abstract

In this study, temperature-resistant functional monomer (TEPA) and hydrophobically associating salt-resistant monomer (APC) were synthesized, respectively. These functional monomers were polymerized with acrylamide (AM) and acrylic acid (AA) to prepare a temperature-resistant and salt-resistant polyacrylamide oil displacement agent with siloxane groups. The viscosity of quaternary copolymer (AATA) solution was taken as evaluation index, the optimum polymerization conditions were determined by single factor experiment. The structure of AATA was characterized by Fourier-transform Infrared (FTIR), ^{1}H NMR spectroscopy and SEM. The thermal decomposition capability was analyzed by TG. The oil displacement efficiency of AATA was evaluated by core flooding experiment. The results showed that AATA had better oil displacement ability than binary copolymer (AM/AA). The enhanced oil recovery was 19.92% at 60 °C and more than 10% even at 90 °C.

Keywords Temperature-resistant polymer · Organo siloxane group · Dehydration condensation · Enhanced oil recovery

1 Introduction

Global energy markets have become more turbulence and unrest because of coronavirus disease 2019 (COVID-19). Inevitably, oil resources have also been hit badly [1]. However, the global demand for oil energy is still large, and it is even expected to reach a peak by 2030 [2]. Therefore, enhanced oil recovery (EOR) technology is highly valued [3–7]. In addition, polymer flooding technology had a broad prospect with the gradual growth of polymer materials science [8]. Injecting of high-viscosity polymer solution into the formation could improve the oil-water mobility ratio and expand the swept volume, thereby enhancing oil recovery [9]. In addition, under the action of stress field, pressure field and flow velocity field, the viscoelasticity of the polymer solution is improved, so the recovery factor is also improved [10].

✉ Tianhong Zhao
swpuzhaotianhong@163.com

[1] College of Chemistry and Chemical Engineering, Southwest Petroleum University, Chengdu, Sichuan 610500, People's Republic of China

[2] Oil & Gas Field Applied Chemistry Key Laboratory of Sichuan Province, Southwest Petroleum University, Chengdu, Sichuan 610500, People's Republic of China

However, most oil pools with good reservoir conditions have been exploitation by water flooding and polymer flooding for many years, and it was more difficult to increase production steadily. In particularly, the development of high temperature and high salinity reservoirs faced greater difficulties. Since the traditional partially hydrolyzed polyacrylamide (HPAM) was not suitable for high temperature and high salinity reservoirs, it was urgent to find a suitable polymer flooding agent for high temperature and high salinity reservoirs [3, 11–13]. In order to improve the temperature and salt resistance of polyacrylamide solution, scholars have deeply studied the molecular structure [13–17], solution performance and mechanism of polymer flooding agent.

Kujawa et al. [18, 19] introduced 2-acrylamido-2-methylpropanesulfon-ic acid (AMPS) and hydrophobic monomers into macromolecular chains through micellar polymerization, and synthesized polyacrylamide polymers containing strong electrolytes with good viscosification and excellent salt resistance. Charles et al. [20] prepared a series of oil-soluble hydrophobically associating polyacrylamide by copolymerization of N-alkyl acrylamide and AM, which showed better viscosity and salt-resistance than traditional polyacrylamide. Zhang et al. [21] prepared a terpolymer with high viscosity retention at high temperature and salinity by introducing n-vinylpyrrolidone (NVP) and diacetone

acrylamide (DAAM) into polyacrylamide. Wang et al. [22] also introduced the organic siloxane structure into the polyacrylamide oil displacement agent, and the quaternary copolymer with excellent temperature-resistance and salt-resistance were synthesized by copolymerization of vinyltriethoxysilane (VETO), hydrophobic monomer, strong electrolysis monomer and AM. In addition, it was reported that APP4 polymer solution with concentration of 1750 mg/L and viscosity of 351.3 mPa·s could enhance oil recovery by 14.3%. The CAB20 polymer solution with concentration of 1750 mg/L and viscosity of 289.5 mPa·s could enhance oil recovery by 15.9%. The HTPW polymer solution with concentration of 1750 mg/L and viscosity of 78.0 mPa·s could enhance oil recovery by 18.8% [23]. Xu et al. [24] reported that the porosity was 34.1% and the the permeability was 0.2 μm^2, xanthan gum and welan gum could enhance oil recovery by 26.5% and 34.5%, respectively.

The bond energy of Si-O-Si is 452 kJ/mol, which is higher than C-C and C-O bonds [25, 26]. Because the high bond of Si-O-Si can ensure the stability of polymer structure, the performance of polymer can be greatly improved by introducing functional monomers contained organic siloxane into the polymer molecular chain [27]. Therefore, in this paper, a functional monomer contained organic siloxane was designed with acryloyl chloride and 3-aminopropyltriethoxysilane (KH-550), and a siloxane functional polyacrylamide with temperature and salt resistance was synthesized. Because KH-550 was a kind of alkoxysilane, it was easy to hydrolyze into silanol in aqueous solution and the hydrolysis reaction was a chemical equilibrium system of step-by-step dissociation [27–29]. At the same time, intermolecular easy dehydration condensation to form siloxane or polysiloxane (Fig. 1(a)). As the silanol in the linear polyacrylamide molecular chain can undergo intermolecular condensation reaction and the hydrogen bond association of the alcohol hydroxyl group, the micro-crosslinking structure can be formed in the polymer molecular chain (Fig. 1(b)). An increase in the hydrodynamic radius can lead to an increase in viscosity. The steric hindrance effect can inhibit the hydrolysis of the amide group and reduce the viscosity reduction rate [30–32]. In addition, a small amount of APC can improve the salt-resistance of the polymer. The abbreviations used in this paper were shown in Table 1.

2 Experimental Section

2.1 Materials and Instruments

2.1.1 Materials

3-Aminopropyltriethoxysilane (KH-550), sodium dodecyl sulfate (SDS), acryloyl chloride, triethylamine, dichloromethane, acrylamide (AM), acrylic acid (AA), sodium

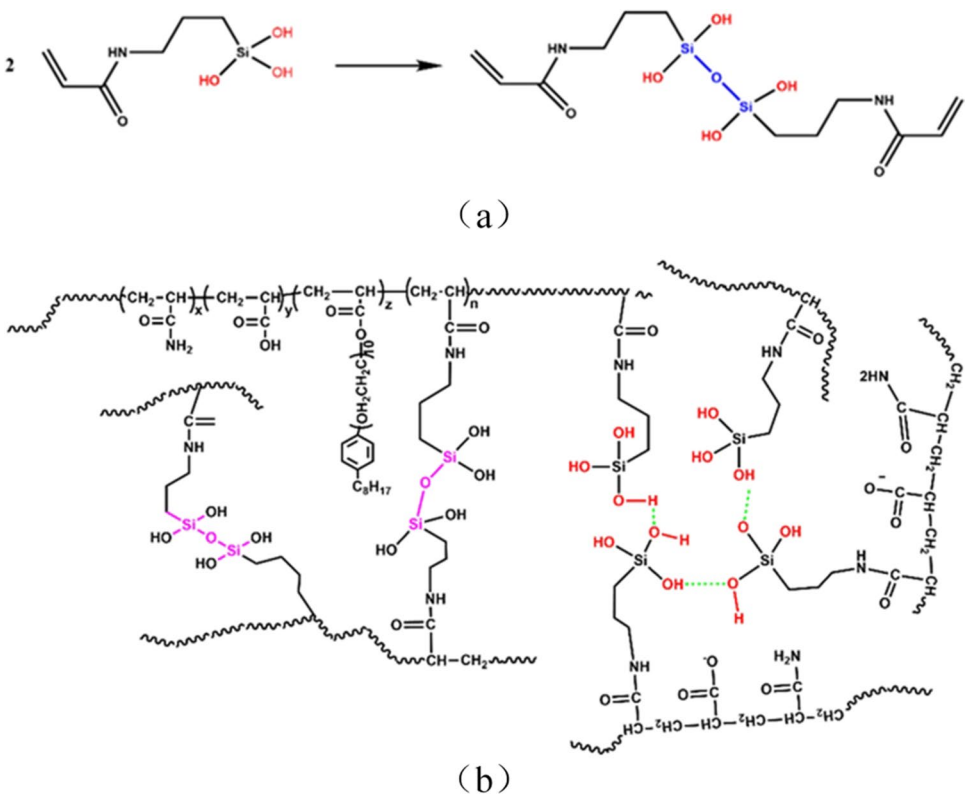

Fig. 1 (**a**) condensation mechanism and (**b**) micro-crosslinking structure of quaternary copolymer

Table 1 List of abbreviations used in the paper

Abbreviation	Full name
AA	Acrylic acid
AATA	The synthesized quaternary copolymer
AM	Acrylamide
AMPS	2-Acrylamido-2-methyl-propanesulfon-ic acid
AM/AA	Binary copolymer
APC	Salt-resistant monomer
DAAM	Diacetone acrylamide
EOR	Enhanced oil recovery
FTIR	Fourier-transform infrared spectroscopy
G′	Elastic modulus
G″	Viscous modulus
^{1}H NMR	^{1}H NMR spectroscopy
HPAM	Partially hydrolyzed polyacrylamide
KH550	3-Aminopropyltriethoxysilane
KYPAM	Salt-resistant comb-like acrylamide polymers
NVP	N-vinylpyrrolidone
OP-10	Dodecane phenol polyoxyethylene ether
SDS	Sodium dodecyl sulfate
SEM	Scanning electron microscope
TEPA	(3-Methacrylamidopropyl)triethoxysilane
TG	Thermal gravimetric
VETO	Vinyltriethoxysilane
V50	2,2-Azobis (2-methylpropamidine) dihydrochloride

hydroxide, 2,2-azobis (2-methylpropamidine) dihydrochloride (V50), dodecane phenol polyoxyethylene ether (OP-10) and inorganic salt were purchased from Kelong Chemical Reagent Factory, Chengdu, China. All reagents were analytical reagent. In addition, KYPAM was purchased from Beijing Hengju Co., LTD and its molecular weight is 25 million.

2.1.2 Instruments

MS-TS analytical balance which the accuracy was 0.1 mg, HH-2 constant temperature oil bath pot, RE-201D rotary evaporator, HASUC vacuum drying chamber. Brookfield viscositor DV-II viscometer was purchased from Brookfield, USA. The structure and properties of polymer systems were characterized by Fourier-transform infrared spectroscopy (FTIR), ^{1}H NMR spectroscopy, scanning electron microscope (SEM) and thermal gravimetric analyzer (TGA).

2.2 Synthesis

2.2.1 Synthesis of Functional Monomer TEPA

11.35 g KH-550 was mixed with 60 mL dichloromethane and added to a 500 mL three-necked flask. Then, 7.27 g triethylamine (as acid binding agent) and 40 ml dichloromethane were added to the three-necked flask. The device was put in 0 °C water bath with stirring. Finally, 5 mL acryloyl chloride was dissolved in 20 mL dichloromethane, the solution was added into the three-necked flask drop by drop, and the dripping time was controlled for 20 min. The crude product was obtained after reaction for 3 h. Then, TEPA was obtained by filtration and rotary evaporation of crude products. The synthetic route of TEPA was shown in Fig. 2.

2.2.2 Synthesis of Functional Monomer APC

Zhang et al. [27] introduced the synthesis method of salt-resistant functional monomer APC. 120 ml dichloromethane, 20 g OP-10 and 7.3 g triethylamine (as acid binding agent) were added in a 500 ml three-necked flask. Afterwards, 5 ml acryloyl chloride and 20 ml dichloromethane were mixed evenly and added in the three-necked flask. The reaction was carried out at 0 °C for 6 h. After that, triethylamine hydrochloride was removed by filtration, and the filtrate was washed repeatedly with acetone. APC was obtained by rotary evaporation. The synthetic route of APC was shown in Fig. 3.

2.2.3 Synthesis of AATA Quaternary Copolymer

Appropriate amount of APC, pure water and SDS were added into a beaker in turn, and the clear and transparent solution was obtained after ultrasonic stirring. A certain amount of AM and AA were successively added to the solution, and the pH was adjusted with 15 wt% NaOH solution. A certain amount of TEPA was added to the system and stirred well. The V50 was added after a water bath for 20–30 min. Some gel-like polymer products were obtained after a certain reaction time. The product was cut into pieces (volume less than 0.5 cm^3) and placed in a 60 °C constant temperature oven to dry. The synthetic route of AATA was shown in Fig. 4.

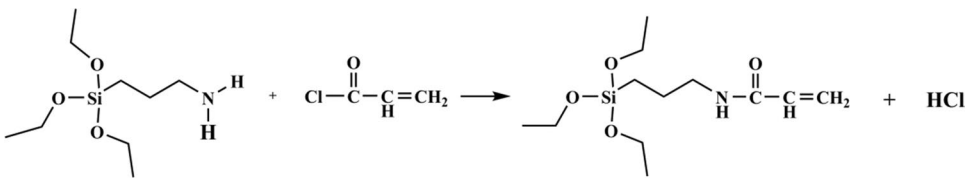

Fig. 2 Synthetic route of the functional monomer TEPA

Fig. 3 Synthetic route of the salt resistant monomer APC

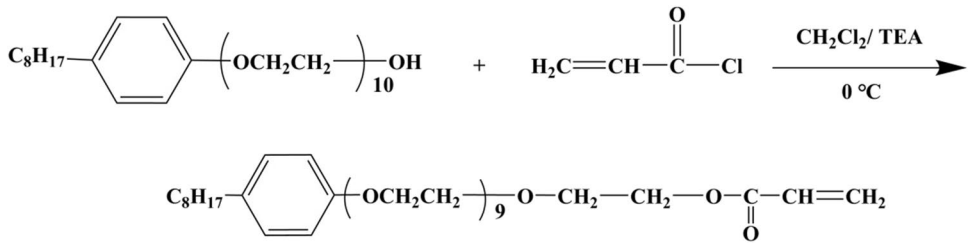

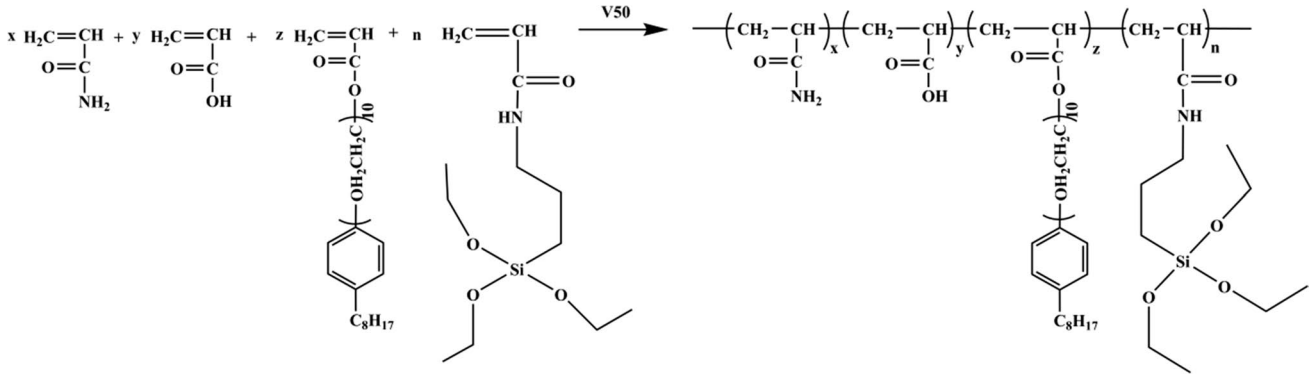

Fig. 4 Synthetic route of the AATA

Table 2 Simulated water parameters

Na^+ (mg/L)	Ca^{2+} (mg/L)	Mg^{2+} (mg/L)	Cl^- (mg/L)	Total mineralizatio (mg/L)
64620	10000	2000	123380	2×10^5

2.3 Performance Evaluation of AATA Quaternary Copolymer Solution

2.3.1 Evaluation of Temperature-Resistance

The viscosity of the polymer solution at different temperatures (25 °C to 85 °C) was measured by the Brookfield viscositor DV-II viscometer. The effect of temperature on the viscosity of polymer solution was investigate.

2.3.2 Evaluation of Salt-Resistance

The viscosity changes of different polymer systems under Na^+, Ca^{2+}, Mg^{2+} and different mineralization degree simulated water conditions were investigated at fixed temperature and concentration. The composition of simulated water was shown in Table 2. The different mieralization degree solution was diluted according to the formula.

2.3.3 Evaluation of Anti-Aging

Three different types of acrylamide polymer solution were placed in 90 °C oven for 90 days, and their viscosity was regularly tested. The anti-aging of different types of polymer solution at 90 °C were investigated.

2.3.4 Evaluation of Shear-Resistance

The viscosity changes of AATA solution, AM/AA solution and KYPAM solution at different shear rates ($0.1\ s^{-1} \sim 1000\ s^{-1}$) were investigated.

2.3.5 Evaluation of Viscoelasticity

Dynamic shear flow experiments were carried out on three different types of polymer solutions at 25 °C to investigate the viscoelasticity of three different types of polymer solutions.

2.4 Core Flooding Experiment

The oil displacement efficiency of AATA was evaluated at 60 °C, 75 °C and 90 °C. The oil displacement efficiency of AATA and AM/AA were compared at 60 °C. In addition, the mineralization degree of simulated water used in oil displacement experiment was 1×10^5 mg/L. The flow chart of core flooding experiment was shown in Fig. 5 and the core parameters were shown in Table 3.

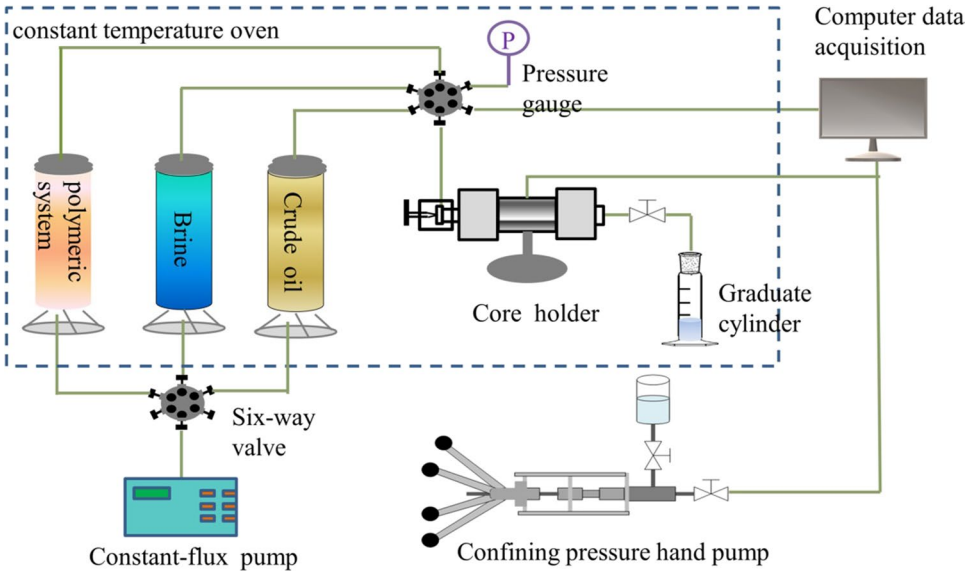

Fig. 5 Schematic flow diagram for the flooding system

Table 3 Core parameters for flooding experiment

Core	Diameter (cm)	Length (cm)	Dry weight (g)	Wet weight (g)	Permeability (mD)
#1	3.820	7.252	144.78	164.19	95.10
#2	3.816	7.273	145.43	164.74	94.66
#3	3.816	7.302	161.37	179.32	94.96
#4	3.821	7.326	146.29	165.58	95.39

3 Results and Discussion

3.1 Single Factor Experiment

In this paper, the viscosity of copolymer solution with concentration of 2 g/L was used as the single factor evaluation basis to explore the influence of various factors on the viscosity of polymer. As can be seen in Fig. 6, the optimal concentrations of SDS, initiator, AA and TEPA were 1.4 wt%, 0.08 wt%, 4 wt% and 0.02 wt%, respectively. When the reaction temperature was 55 °C and the reaction time was 6 h, the viscosity of the polymer was highest. Meanwhile, the best monomer concentration was 20 wt%.

3.2 Characterize

3.2.1 FTIR and ^{1}H NMR Spectroscopy Analysis of TEPA

As shown in Fig. 7(a), the chemical structure of KH-550 and TEPA was characterized by FTIR. Among them, 2975 cm^{-1} and 2940 cm^{-1} were the asymmetric stretching vibration peaks of -CH_3 and -CH_2, respectively [33]. The symmetric stretching vibration peaks of Si-O bond at 462 cm^{-1} and 754 cm^{-1}. Otherwise, the asymmetric vibration peak of Si-O-C was at 1041 cm^{-1}, and the symmetric vibration peaks of Si-O-C were at 800 cm^{-1} and 700 cm^{-1}. By comparing the spectra of KH-550 and TEPA, the characteristic peaks of C-N (1405 cm^{-1}), C=C (1621 cm^{-1}), C=O (1664 cm^{-1}), N-H (stretching vibration peak at 3286 cm^{-1} and bending vibration peak and 1554 cm^{-1}) were found in TEPA. These proved that TEPA was successfully synthesized.

^{1}H NMR (400 MHz, D_2O, 25 °C) of TEPA spectra with its chemical shifts were as follows; the chemical shift signal at 4.70 ppm was ascribed to the protons of D_2O. The signal of the protons in $-O-CH_2-$ was 2.30 ppm, the signal of the protons in $-CH_3$ was 0.80 ppm [34]. The signal of the protons in $-Si-CH_2-$ was 0.25 ppm, the signal of the protons in $-CH_2-$ was 1.41 ppm, the signal of the protons in $-CH_2-N-$ was 3.04 ppm, and the signal of the proton in $-NH-$ was 5.56 ppm [35]. The chemical shifts at 5.99 ppm and 6.07 ppm were respectively ascribed to the protons of $-CH_2-$ at the end and $-CH-$ in the propylene [36, 37].

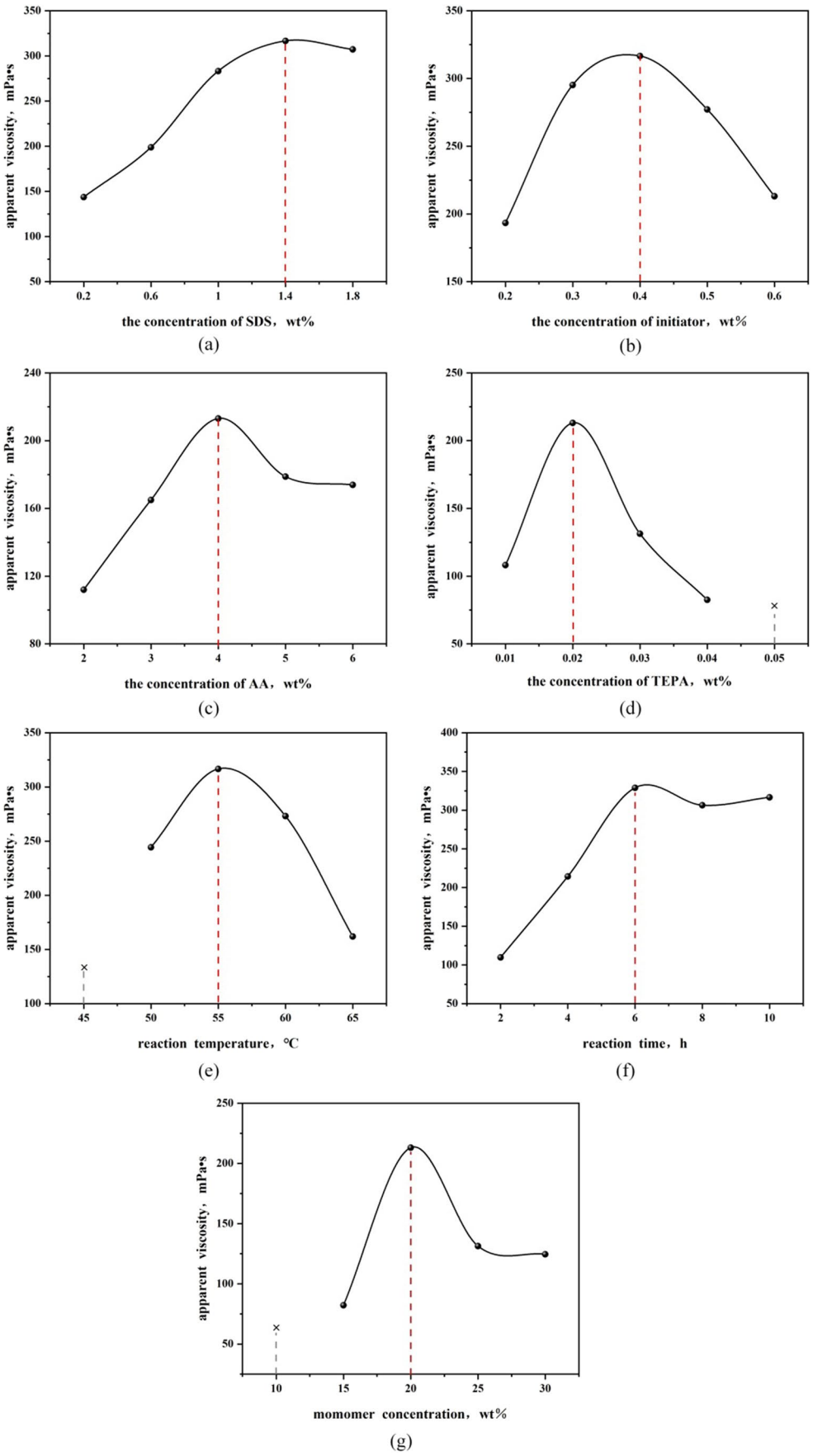

Fig. 6 Effects of synthetic factors on the solution viscosity of AATA

3.2.2 FTIR and ^{1}H NMR Spectroscopy Analysis of AATA

As can be seen from Fig. 8(a), there were symmetric stretching vibration absorption peak (2923 cm^{-1}) and antisymmetric stretching vibration absorption peaks (2851 cm^{-1}) of C-H in methylene [38]. The stretching vibration peak and bending vibration peak of N-H in amide were at 3182 cm^{-1} and 1550 cm^{-1}, respectively. The stretching vibration absorption peak of C=O in amide was at 1683 cm^{-1}. The stretching vibration absorption peak of Si-O at 1122 cm^{-1} was the characteristic peak of TEPA, which proved that TEPA was successfully introduced into AATA. The stretching vibration peak of C=C in benzene ring at 1517 cm^{-1} and the out-of-plane bending vibration peak of C-H on benzene ring at 817 cm^{-1} were both characteristic peaks of APC, which preliminarily proved that APC was successfully introduced into AATA.

In order to further study the structure of AATA, ^{1}H NMR analysis was studied. The results were shown in Fig. 8(b). ^{1}H NMR (400 MHz, D_2O, 25 °C) of AATA spectra with its chemical shifts were as follows; the chemical shift signal at 4.70 ppm was ascribed to the protons of D_2O. The chemical shifts at 1.86 ppm and 2.00 ppm were respectively attributed to the protons of $-CH_2-$ and $-CH-$ on macromolecular main chains, revealed a characteristic broad resonance of the hyperbranched groups [39, 40]. $-O-CH_2-CH_2-O-$ were detected at 3.48 ppm [41, 42]. The signals at 1.39 ppm can be assigned to $–CH_2–ph–$ [43]. The chemical shift signal at 1.01 ppm was ascribed to the protons of $–CH_3$.

In summary, the analysis of FTIR and ^{1}H NMR showed that AATA was successfully synthesized.

3.2.3 Microstructure of AATA

To investigate the properties of AATA deeply, the microstructure was analyzed. As can be seen from Fig. 9, the microstructure of AATA solution showed an obvious network structure, which was caused by the hydrogen bond association in TEPA, the condensation between silanols, the formation of Si-O-Si structure and the hydrophobic association of APC.

3.2.4 Thermal Stability Analysis of AATA

Due to the high formation temperature, it is necessary to analyze the thermal stability of polymer to avoid high-temperature abatement [44–47]. Firstly, the thermal gravigrams of three different types of polymers were compared. Figure 10(a) showed that the heat loss weight of AATA was lower than AM/AA in the temperature range of 40 °C ~ 423 °C and 530 °C ~ 600 °C. At the same time, the heat loss of AATA was less than KYPAM in the temperature range of 40 °C ~ 224 °C, 277 °C ~ 414 °C and 519 °C ~ 600 °C.

As is shown in Fig. 10(b), with the increase of temperature, the copolymer appeared four weight loss stages. 41 °C ~ 168 °C was the first weight loss stage, and the copolymer lost 7.25% due to evaporation of water. The second weight loss stage was at 212 °C ~ 235 °C, and the weight loss of copolymer was 10.6%, which was mainly due to the cracking of condensation products between amide groups in the molecular chain. 289 °C ~ 295 °C was the third weight loss stage, and the heat loss caused by the pyrolysis of polymer branched chain was 14.25%. The fourth stage occurred at 295 °C ~ 444 °C, the weight loss was 19.26%, which was due to the macromolecular chain fracture and the carbonization of the copolymer.

3.3 Performance Evaluation of AATA Solution

3.3.1 Viscosity Enhancement Evaluation

In this paper, the viscosity of three different types of polymer solution as a function of concentration was studied. As shown in Fig. 11, the viscosity of the three polymer solution increased with the increase of concentration. At the same concentration, the viscosity of AATA and KYPAM were higher than AM/AA. Because AATA contained organic siloxane functional monomer, the siloxane structure in aqueous solution was hydrolyzed to form silanol, and dehydration condensation reaction occurred, so that the polymer microstructure was grid-like, so its viscosity was higher [48]. The hydrophobic group and hydrophilic group in KYPAM molecular chain repelled each other, resulting in larger hydrodynamic radius than AM/AA. So its viscosity was higher, and the viscosity difference was more obvious with the increase of concentration [49, 50].

3.3.2 Evaluation of Temperature-Resistance

AATA, AM/AA and KYPAM solution with concentration of 2 g/L were prepared with pure water. The viscosity at different temperatures was measured. As shown in Fig. 12(a), with the increase of temperature, the viscosity of three types of polymer solution showed a downward trend, and the viscosity of AATA solution decreased most slowly. As can be seen in Fig. 12(b), the viscosity retention rate of AATA solution was the highest (73.14%), and AM/AA solution was only 51.72% at 85 °C.

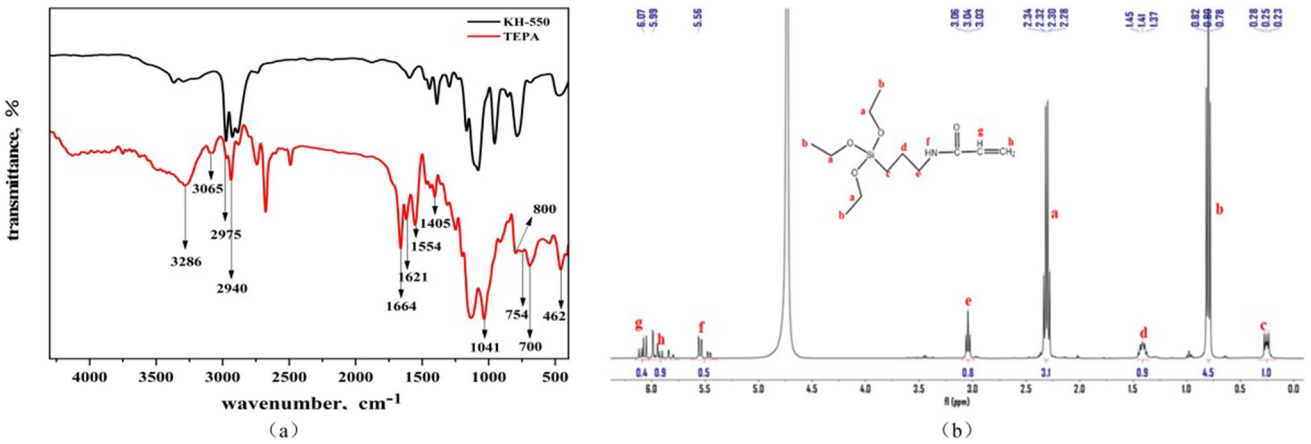

Fig. 7 FTIR spectra and ^{1}H NMR spectrum of TEPA

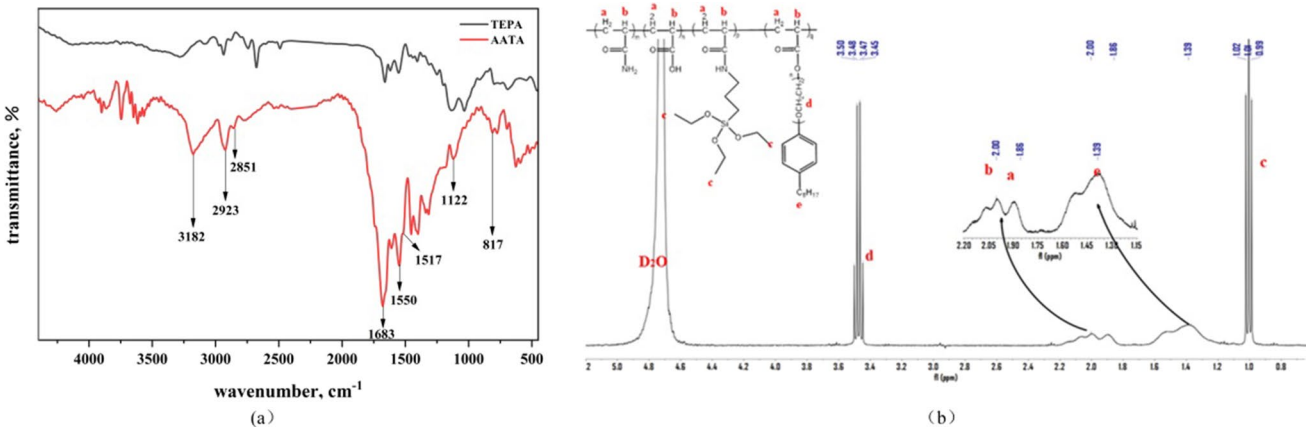

Fig. 8 FTIR spectra and NMR spectrum of AATA

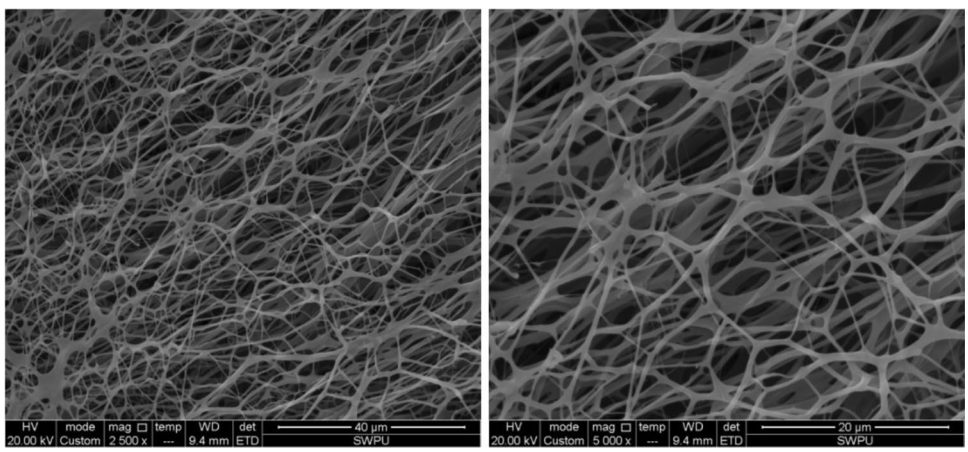

Fig. 9 The microstructure of AATA

3.3.3 Evaluation of Salt-Resistance

Since Na^{+}, Ca^{2+} and Mg^{2+} can occur charge shielding effect with carboxylic acid groups, the viscosity of polymer solution can be reduced [51]. Therefore, it is necessary to study the salt-resistance of polymer solution. In this paper, the effects of the Na^{+}, Ca^{2+}, Mg^{2+} and different mineralization degree simulated water conditions on the viscosity of copolymer solution were investigated.

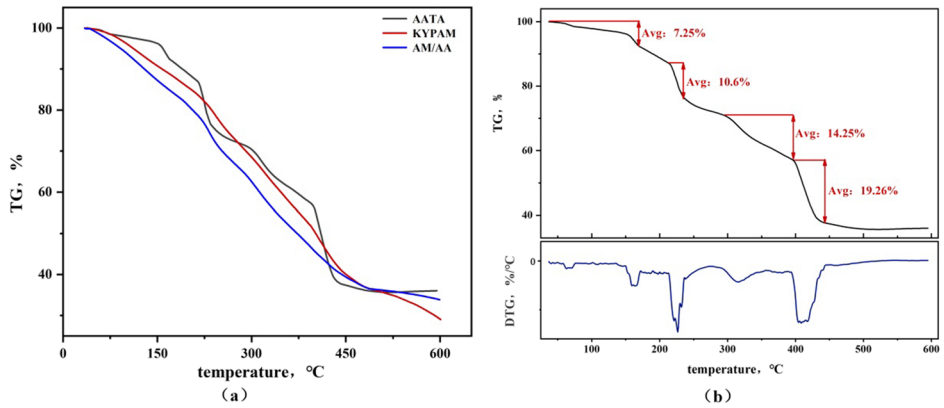

Fig. 10 (**a**) Comparison of TG spectra of three different types of polymers and (**b**) TG-DTG spectra of AATA

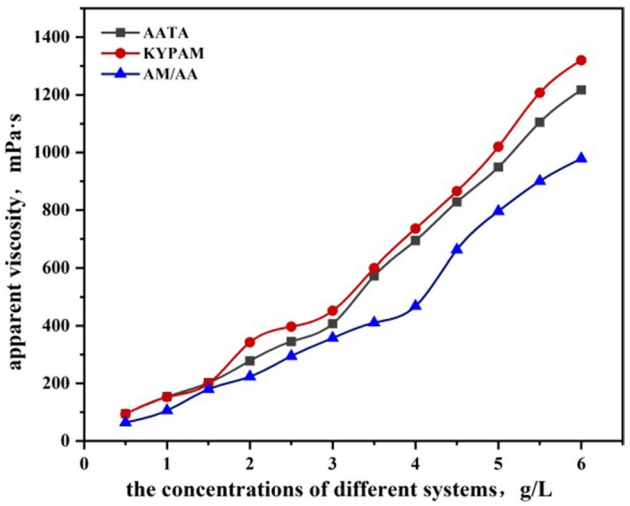

Fig. 11 Viscosity - concentration curves of different types of polymers

As shown in Fig. 13, with the increase of Na^+, Ca^{2+} and Mg^{2+} concentration, the viscosity of AM/AA solution and KYPAM solution decreased significantly. When the concentration of Na^+ was 3×10^5 mg/L, the viscosity of KYPAM solution and AM/AA solution was very small, only 8.75 mPa·s and 7.32 mPa·s, respectively. However, with the increase of Na^+, the viscosity of AATA solution increased first and then decreased. When the concentration of Na^+ was 1.6×10^5 mg/L, the viscosity reached the highest (869.9 mPa·s). It was possibly due to the role of APC in the polymer, the increase of cation concentration enhanced the solution polarity and the hydrophobic association between molecules made the polymer form a more stable network structure so that the solution viscosity increased. The viscosity of the polymer solution began to decrease after the concentration of Na^+ exceeded 1.6×10^5 mg/L, which was due to the saturation of the ability of ethoxy to complexation metal ions at high salinity. The metal ions that failed to complexation were combined with the anionic groups, which inhibited the mutual repulsion between the anionic groups and made the polymer molecular chain easy to curl. In addition, since the charge of Ca^{2+} and Mg^{2+} was twice as much as Na^+, the electrostatic shielding effect on carboxylate was stronger, so the decreasing trend of viscosity was more obvious.

Since the strata water was very complex which contained a variety of cations, it was necessary to study the influence of different mineralization degree on the polymer solution. As shown in Fig. 13(d), AATA has better mixed salt-resistance than KYPAM and AM/AA. When the mineralization degree of simulated water was 2×10^5 mg/L, the viscosity of

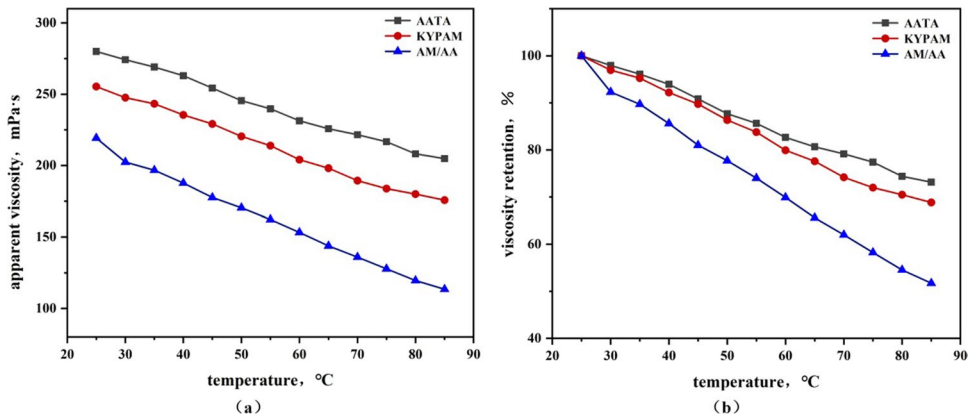

Fig. 12 (**a**) Temperature-viscosity curves of three types of polymer solution and (**b**) temperature- viscosity retention rate curves of three types of polymer solution

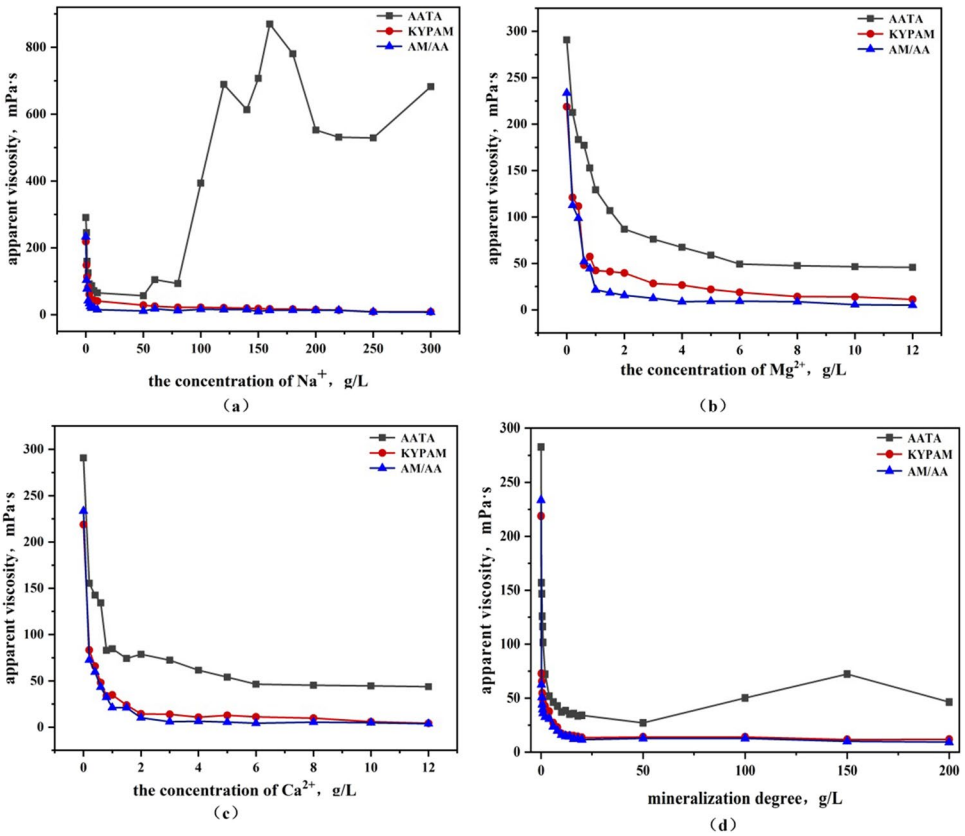

Fig. 13 Salt-resistance of three polymer solution (**a**) Na^+ concentration-viscosity curves, (**b**) Mg^{2+} concentration-viscosity curves, (**c**)Ca^{2+} concentration-viscosity curves and (**d**) mineralization degree concentration-viscosity curves

AATA was 46.43 mPa·s, while the viscosity of KYPAM was only 11.79 mPa·s, and AM/AA was lower, only 9.27 mPa·s. This was due to the hydrophobic association and dehydration condensation of APC and TEPA in AATA to form a network structure, which made AATA maintain higher viscosity.

3.3.4 Evaluation of Anti-Aging

In order to meet the needs of reservoir, this paper studied the viscosity change of polymer solution under high temperature for a long time. Figure 14(a) showed that the viscosity of the three polymer solution decreased significantly on the first seven days and remained basically unchanged after 30 days. On the 90th day, the viscosity of AATA was 47.89 mPa·s, and the viscosity retention rate was 19.23%, which were higher than KYPAM and AM/AA. The reason may be that there was Si-O-Si structure in AATA, and the bond energy of Si-O bond was higher than C-O and C-C, the stability was stronger. Therefore, the viscosity loss of the AATA was smaller at high temperature.

As shown in Fig. 14(b), the viscosity of AATA showed the same trend with time under different temperature conditions. On the 90th day, the viscosity retention rate of AATA was the highest at 45 °C, reached 72.34%, while it

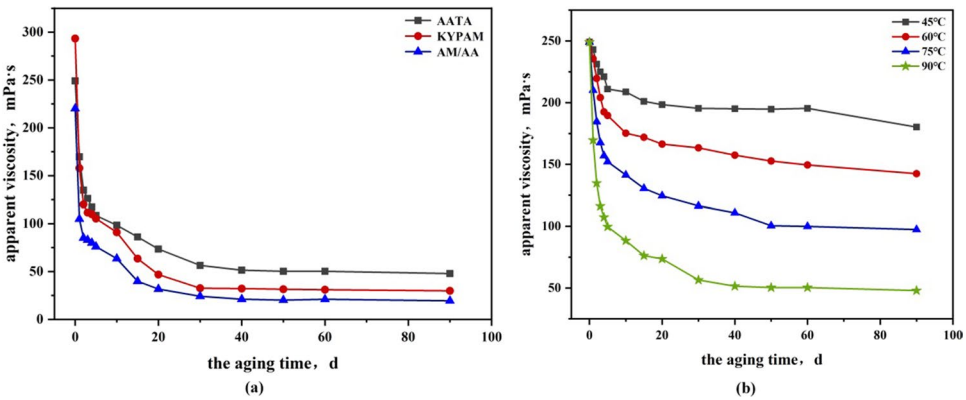

Fig. 14 (**a**) Viscosity changes of three types of polymers solutions with aging time at 90 °C and (**b**) the viscosity of AATA changes with aging time at different temperatures

was only 19.23% at 90 °C. It showed that the higher the temperature, the faster the oxidative degradation rate of the polymer, the more serious the viscosity loss.

3.3.5 Evaluation of Shear-Resistance

AATA, KYPAM and AM/AA solution with the same concentration (2 g/L) were prepared with pure water to observe the viscosity changes at different shear rates (0.1 s^{-1} ~1000 s^{-1}). With the increase of shear rate, shear thinning occurred in all the polymer solution (Fig. 15). When the shear rate was 1000 s^{-1}, the viscosity retention rate of KYPAM was the smallest (0.1%), and AM/AA was 0.26%. At the same time, the viscosity retention rate of AATA was the largest (2.75%). This indicated that AATA had stronger shear-resistance under the same conditions. In conclusion, the decrease trend of viscosity at the same shear rate was KYPAM > AM/AA > AATA.

3.3.6 Viscoelasticity Evaluation

Viscoelasticity had an important impact on the properties of polymer solution. Therefore, the dynamic shear experiment was carried out at 25 °C. AATA, AM/AA and KYPAM solution with concentration of 2 g/L were prepared with pure water. As shown in Fig. 16(a), the elastic modulus (G′) and the viscous modulus (G″) of three polymer solution increased with the increase of the oscillation frequency. The G′ of AATA and KYPAM was always greater than the G″, indicating that AATA and KYPAM were always dominated by elasticity in the dynamic shear flow experiment. The G′ of AATA was always higher than AM/AA, indicating that the viscoelasticity of AATA was stronger.

Dynamic shear flow experiments were carried out at 25 °C, 45 °C and 80 °C to investigate the effect of temperature on the viscoelasticity of AATA. As shown in Fig. 16(b), at 25 °C and 45 °C, the G′ of AATA was greater than G″, the elasticity was dominant and the G″ was greater than G′ at 80 °C, the viscosity was dominant. Due to the higher elasticity, the polymer solution could bring more crude oil through deformation in the process of oil displacement, so the polymer solution had better oil displacement effect at lower temperature.

3.4 Flooding

3.4.1 Oil Displacement Effects of Two Polymer Systems

The oil displacement effects of AM/AA and AATA were compared at 60 °C. As shown in Fig. 17, AM/AA can

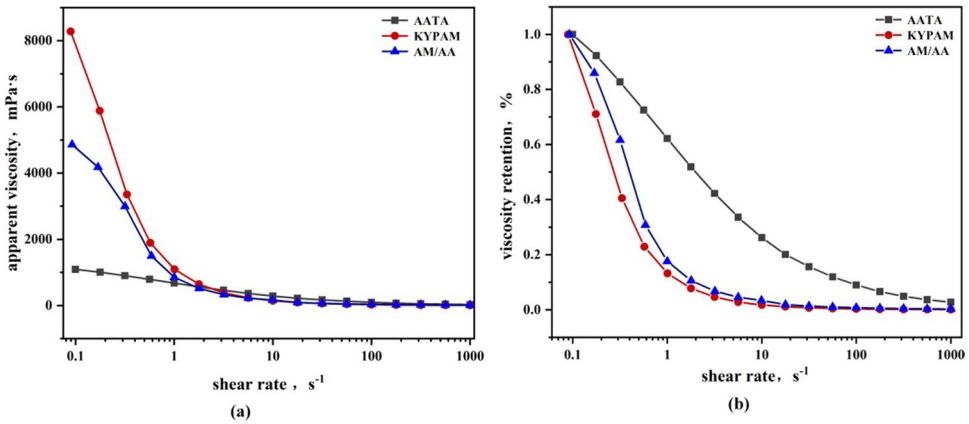

Fig. 15 (**a**) Viscosity changes of three types of polymers solutions with shear rate and (**b**) viscosity retention changes of three types of polymers solutions with shear rate

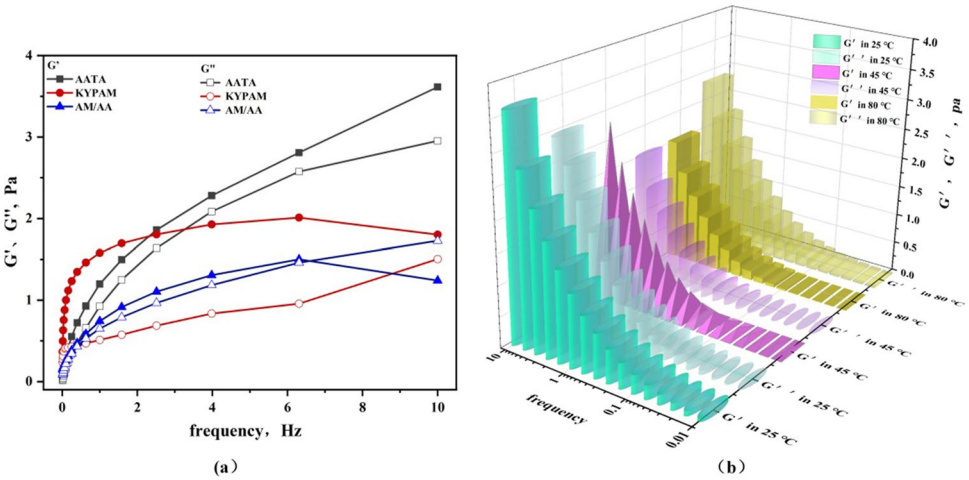

Fig. 16 (**a**) Effect of oscillation frequency on viscoelasticity of three different polymer solution and (**b**) effect of oscillation frequency on viscoelasticity of AATA at different temperatures

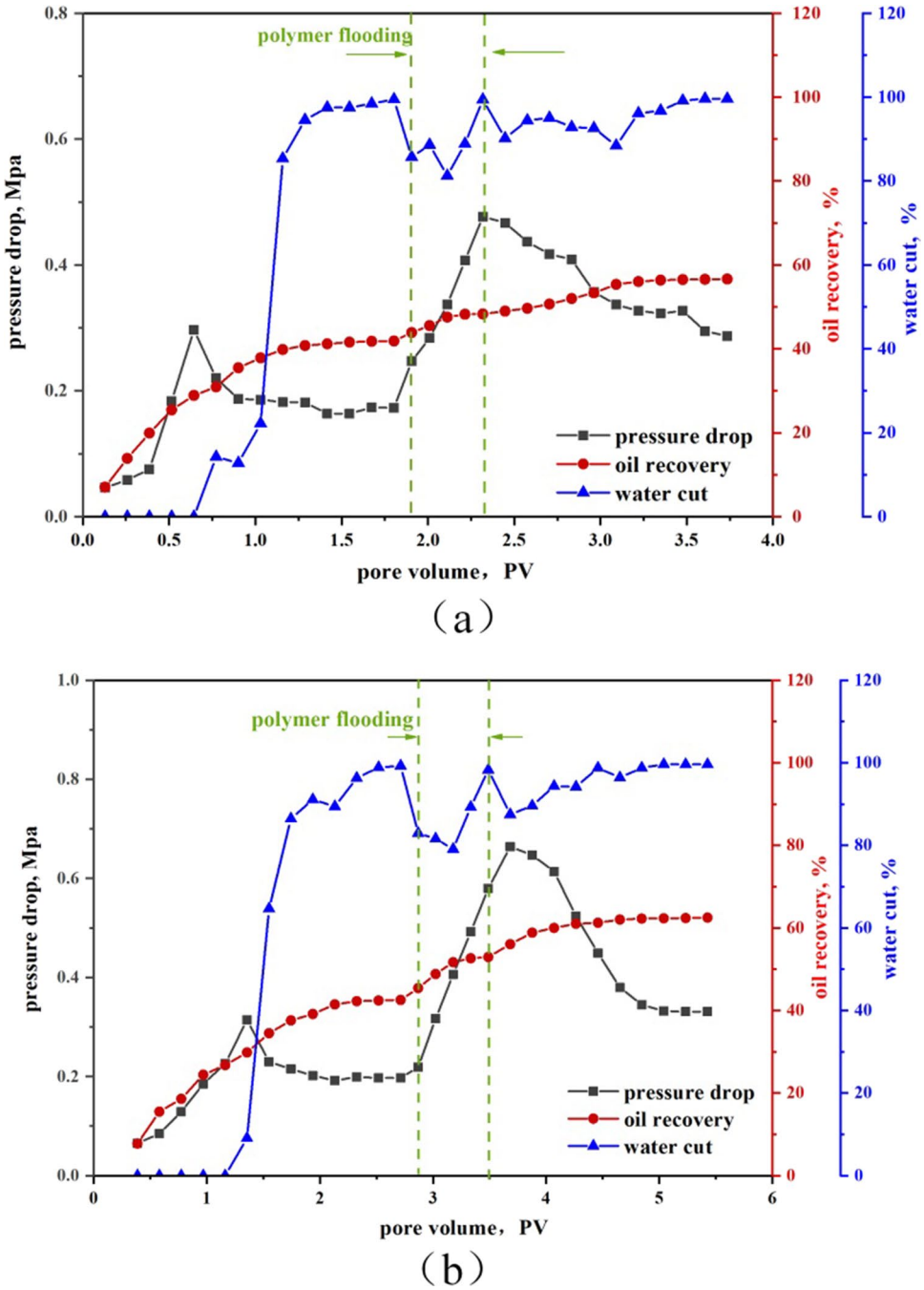

Fig. 17 Oil displacement performance of two polymer systems at 60 °C and 1×10^5 mineralization degree (**a**) AM/AA flooding and (**b**) AATA flooding

Table 4 Oil displacement performance of AATA various temperatures

Temperature(°C)	Water drive recovery efficiency (%)	Recovery factor of polymer flooding (%)	Subsequent water flooding recovery factor (%)	EOR (%)
60	42.56	10.29	9.54	19.92
75	40.1	8.64	7.69	16.33
90	42.37	5.66	6.77	12.33

enhance oil recovery by 14.77%, and AATA can enhance oil recovery by 19.92%, 5.15% higher than AM/AA. The reason was that the viscosity of AATA solution was higher than AM/AA solution under the same conditions due to the hydrogen bond association and dehydration condensation of silanol in AATA. Therefore, under the same permeability conditions, AATA had stronger ability to control the flow ratio, which can better suppress the fingering phenomenon of injection water and improve the sweep efficiency. Also, AATA had better viscoelasticity and can carry more crude oil in pores through deformation, so as to further enhance oil recovery.

3.4.2 Oil Displacement Effects of AATA at Various Temperatures

The oil displacement efficiency of AATA was measured at 60 °C, 75 °C and 90 °C, respectively. The injection rate was 0.5 mL/min. 2 PV simulated water, 0.5 PV AATA solution and 2 PV subsequent simulated water were successively injected.

As shown in Table 4 and Fig. 18, elevated temperature had adverse effect on polymer flooding efficiency. At 60 °C, AATA can improve the recovery by 19.92%. With the temperature increased, the recovery decreased significantly. This was due to the low viscosity of AATA affected by high temperature and the poor ability to improve the fluidity ratio, resulting in decrease in recovery. However, because AATA had a certain temperature and salt resistance, it still showed a good oil displacement effect at 90 °C, and the enhanced oil recovery reached 12.33%.

4 Conclusions

In summary, the temperature-resistant monomer TEPA contained siloxane functional group and the hydrophobically associating salt-resistant monomer APC were successfully designed and synthesized. TEPA, APC, AM and AA were copolymerized to obtain AATA quaternary copolymer by micelle polymerization. The structures of TEPA and AATA were characterized by FTIR and ^{1}H NMR, which confirmed that TEPA and APC were successfully introduced into the copolymer molecular chain. SEM showed that AATA had obvious network structure. Thermogravimetric analysis showed that AATA had better resistance to high thermal decomposition. The oil displacement experiment showed that the oil displacement efficiency of AATA was better than AM/AA under the same conditions, and the oil recovery can still be increased by 12.33% at 90 °C. It indicated that AATA as an oil displacement agent had good ability to enhance oil recovery. In short, these results showed that AATA had the possibility of application in high temperature and high salinity reservoirs with temperature of 90 °C and salinity of 2×10^{5} mg/L.

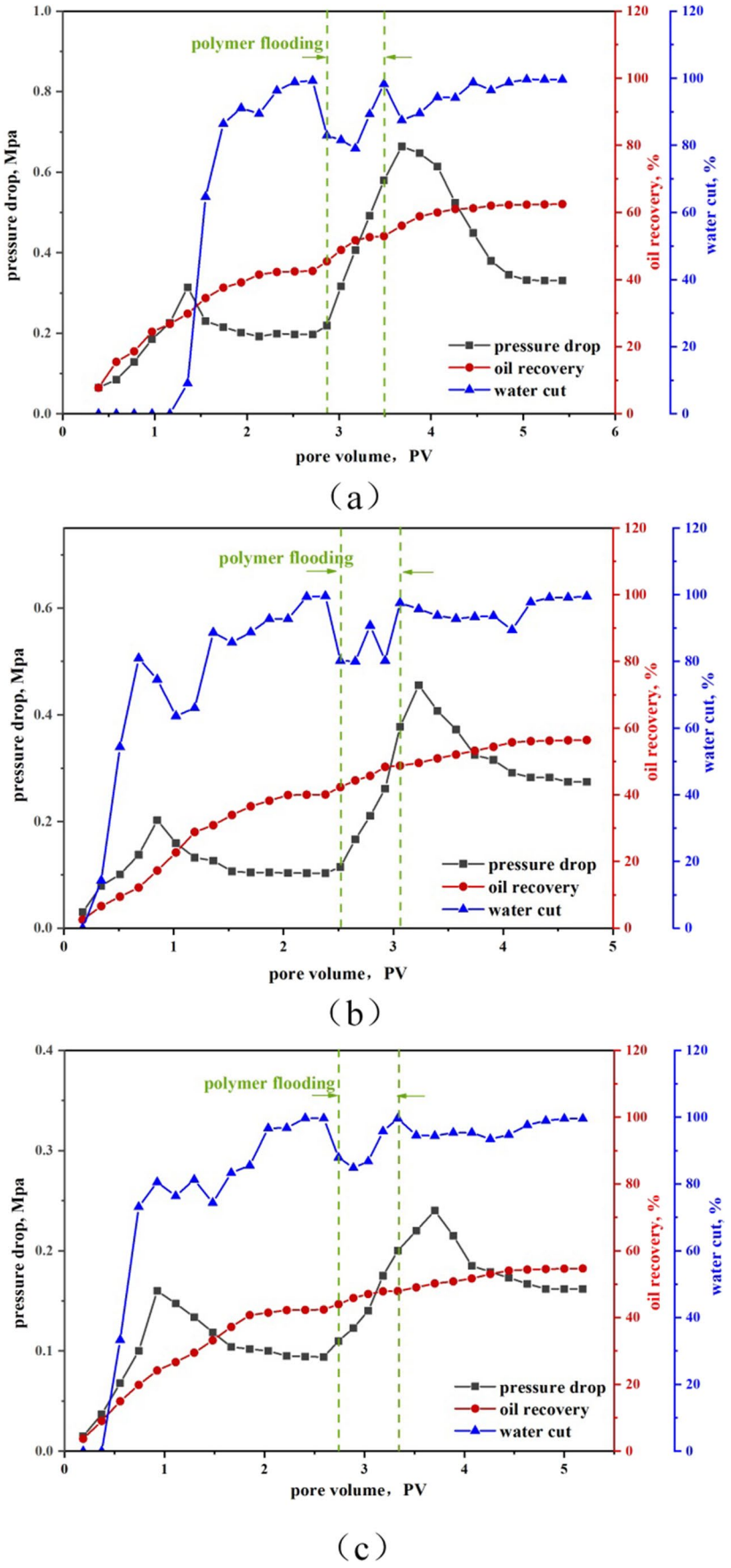

Fig. 18 Oil displacement performance of AATA at 1×10^5 mineralization degree and various temperatures (**a**) at 60 °C (**b**) at 75 °C and (**c**) at 90 °C

Acknowledgments We would like to thank the relevant researchers who provided help during the experiment.

Authors' Contributions Tianhong Zhao: conceptualization, supervision, funding acquisition;

Qiongqiong Guo: data curation, formal analysis, writing - review &editing;

Sijia Li: Methodology; project administration; resources;

Wushan Sun: software; writing - original draft.

Funding This research was supported by "Opening Project of Oil & Gas Field Applied Chemistry Key Laboratory of Sichuan Province, NO: YQKF202006".

Data Availability Data and materials supporting the research are found within the manuscript. Raw data files will be provided by the corresponding author upon request.

Declarations

Ethics Approval The submitted work should be original and should not have been published elsewhere in any form or language (partially or in full).

Consent to Participate Yes.

Consent for Publication Yes.

Competing Interests The authors declare that they have no known competing financial interests or personal relationships that could have appeared to influence the work reported in this paper.

References

1. Xuening. L., Fusheng, Z., Guoliang, L.: Review on polymer flooding technology. IOP Conf. Ser: Earth. Environ. Sci. **675**(1)), 012199 (2021)
2. Fu, X., Qin, F., Liu, T., et al.: Enhanced oil recovery performance and solution properties of hydrophobic associative xanthan gum. Energy Fuels **36**, 181–194 (2022)
3. Li, S., Braun, O., Lauber, L. et al.: Enhancing oil recovery from high–temperature and high–salinity reservoirs with smart thermoviscosifying polymers: a laboratory study. Fuel. **288**, 119777 (2021)
4. Tao, L.: EOR pilot test using AMPS polymer flooding in high temperature reservoirs. J. Oil Gas Technol. **33**(9), 141–144 (2011)
5. Ramkumar, M., Nagarajan, R., Santosh, M.: Reservoir characterization and enhanced oil recovery: Preface. Energy Geosci. **2**, 285–286 (2021)
6. Yuliansyah, A.T., Murachman, B., Purwono, S.: Mathematical model for water flooding and HPAM polymer flooding in enhanced oil recovery. ASEAN J. Chem. Eng. **21**(1), 124 (2021)
7. Zhao, T., Guo, Q., Sun, W., et al.: Synthesis and oil displacement performance evaluation of cation-nonionic gemini surfactant. Colloids Surf. A Physicochem. Eng. Asp. **647**, 129106 (2022)
8. Mahajan, S., Yadav,. H, Rellegadla, S., et al.: Polymers for enhanced oil recovery: fundamentals and selection criteria revisited. Appl. Microbiol. Biotechnol. **105**(21–22), 8073–8090 (2021)
9. Yu, W., Feng, Y., Wang, B., et al.: A novel thermoviscosifying water-soluble polymer: synthesis and aqueous solution properties. J. Appl. Polym. Sci. **116**(6), 3516–3524 (2010)
10. Lin, Y., Huang, R.: Study of P(AM-NVP-DMDA) hydrophobically associating water-soluble terpolymer. J. Appl. Polym. Sci. **74**(1), 211–217 (2015)
11. Jouenne, S.: Polymer flooding in high temperature, high salinity conditions: selection of polymer type and polymer chemistry, thermal stability. J. Pet. Sci. Eng. **195**(4), 107545 (2020)
12. Wu, Z., Xa, Y., Cheng, T., et al.: Effect of viscosity and interfacial tension of surfactant–polymer flooding on oil recovery in high-temperature and high-salinity reservoirs. J. Petrol. Exploration Prod. Technol. **4**, 9–16 (2014).
13. Wang, G., Yi, X., Feng, X., et al.: Synthesis and study of a new copolymer for polymer flooding in high-temperature, high-salinity reservoirs. Chem. Technol. Fuels Oils **48**(2), 112–119 (2012)
14. Zhong, C., Zhang, H., Feng, L.: Solution behavior and associating structures of a salt-tolerant tetra-polymer containing an allyl-capped macromonomer. J. Polym. Res. **21**(12), 604 (2014)
15. Liu, R., Pu, W.F., Peng, Q. et al.: Synthesis of AM-co-NVP and thermal stability in hostile saline solution. Adv. Mater. Res. **602–604**, 1349–1354 (2013)
16. Corpart, J.P., Ernst, B., Liu, F.S.: Synthesis and characterization of fluorine containing hydrophobically associating polymers. Oil Gas Sci. Technol. **52**(2), 231–234 (2006)
17. Zhou, Z., Kang, W., Yang, H., et al.: Synthesis and rheological properties of a Sulfobetaine amphiphilic polymer. J Petrochem Univ **30**(5), 32–36 (2017)
18. Kujawa, P., Rosiak, J.M., Selb, J. et al.: Micellar synthesis and properties of hydrophobically associating polyampholytes. Macromol. Chem. Phys. **202**(8), 1384–1397 (2001)
19. Kujawa, P., Rosiak, J.M., Candau, J.S., et al.: Synthesis and properties of hydrophobically modified polyampholytes. Molecular crystals and liquid crystals science and technology. Section A. Mol. Cryst. Liq. Cryst. **354**(1), 401–407 (2000)
20. McCormick, C.L., Lowe, A.B.: Aqueous RAFT polymeriza-tion: recent developments in synthesis of functional water-soluble (Co) polymers with controlled structures. Acc. Chem. Res. **37**, 312–325 (2004)
21. Zhang, Y., Yan, Y., Guo, Y., et al.: Study of the temperature-resistant and salt-tolerant Terpolymer of Acrylamide (AM), Diacetone Acrylamide (DAAM) and N-Vinyl-2-pyrrolidinone (NVP). Fine Chemicals **23**(5), 494 (2006)
22. Wang, D., Tan, J., Han, Y. et al.: Synthesis and properties of temperature-resistant and salt-tolerant tetra-acrylamide copolymer. J. Macromol. Sci. Part A Chem. **56**(12), 1148–1155
23. Lu, X., Cao, B., Xie, K., et al.: Enhanced oil recovery mechanisms of polymer flooding in a heterogeneous oil reservoir. **48**(1), 169–178 (2021)
24. Xu, L., Xu, G., Yu, L., et al.: The displacement efficiency and rheology of welan gum for enhanced heavy oil recovery. Polym. Adv. Technol. **25**(10), 1122–1129 (2014)
25. Qu, L., Xin, Z.: Preparation and surface properties of novel low surface free energy fluorinated silane-functional polybenzoxazine films. Langmuir. **27**(13), 8365–8370 (2011)
26. Zuo, Y., Liang, X., Yin, J., et al.: Understanding the significant role of Si-O-Si bonds: organosilicon materials as powerful platforms for bioimaging. Coord. Chem. Rev. **447**, 214166 (2021)
27. Zhang, W., Xia, C., Li, L., et al.: Preparation and application of a novel ethanol permselective poly(vinyltriethoxysilane) membrane. RSC Adv. **4**(28), 14592–14596 (2014)
28. Sveistrup, M., Mastrigt, F.V., Norrman, J., et al.: Viability of biopolymers for enhanced oil recovery. J. Dispers. Sci. Technol. **37**, 1160–1169 (2016)
29. Le-Anh, D., Rao, A., Schlautmann, S., et al.: Effects of fluid aging and reservoir temperature on waterflooding in 2.5D glass micromodels. Energy Fuels. **36**, 1388–1401 (2022)
30. Zhao, T., Li, S., Chen, J., et al.: The construction of amphiphilic chemical modified nano silicon dioxide reinforced foam system. J. Pet. Sci. Eng. **205**, 108917 (2021)
31. Coolman, T., Alexander, D,. Maharaj, R., et al.: An evaluation of the enhanced oil recovery potential of the xanthan gum and aquagel in a

heavy oil reservoir in Trinidad. J. Pet. Exploration Prod. Technol. **10**, 3779–3789 (2020)
32. Wu, S.C., Chen, Y.J., Lin, Y.J., et al.: Development of a Mucin4-targeting SPIO contrast agent for effective detection of pancreatic tumor cells in vitro and in vivo. J. Med. Chem. **56**(22), 9100–9109 (2013)
33. Kumar, A., Mandal, A.: Characterization of rock-fluid and fluid-fluid interactions in presence of a family of synthesized zwitterionic surfactants for application in enhanced oil recovery. Colloids Surf. a-Physicochem. Eng. Aspects **549**, 1–12 (2018)
34. El-Hoshoudy, A.N., Desouky, S.E.M., Betiha, M.A., et al.: Use of 1-vinyl imidazole based surfmers for preparation of polyacrylamide-SiO2 nanocomposite through aza-Michael addition copolymerization reaction for rock wettability alteration. Fuel. **170**, 161–175 (2016)
35. Lai, N., Zhu, Q., Qiao, D., et al.: CO2/N-2-responsive nanoparticles for enhanced oil recovery during CO2 flooding. Front. Chem. **8**, 393 (2020)
36. Khalil, M., Fahmi, A., Nizardo, N.M., et al.: Thermosensitive core-shell Fe3O4@poly(N-isopropylacrylamide) Nanogels for enhanced oil recovery. Langmuir. **37**(29), 8855–8865 (2021)
37. Ye, Z., Gou, G., Gou, S., et al.: Synthesis and characterization of a water-soluble sulfonates copolymer of acrylamide and N-allylbenzamide as enhanced oil recovery chemical. J. Appl. Polym. Sci. **128**(3), 2003–2011 (2013)
38. Jia, H., Dai, J., Miao, L. et al.: Potential application of novel amphiphilic Janus-SiO2 nanoparticles stabilized O/W/O emulsion for enhanced oil recovery. Colloids Surf. a-Physicochem Eng. Aspects. **622**, 126658 (2021)
39. Ye, Z., Feng, M., Gou, S., et al.: Hydrophobically associating acrylamide-based copolymer for chemically enhanced oil recovery. J. Appl. Polym. Sci. **130**(4), 2901–2911 (2013)
40. Gou, S.H., Liu, M., Ye, Z.B., et al.: Modification of a nicotinic acid functionalized water- soluble acrylamide sulfonate copolymer for chemically enhanced oil recovery. J. Appl. Polym. Sci. **131**(8), 141 (2014)
41. Bi, Y., Tan, Z., Wang, L., et al.: The demulsification properties of cationic hyperbranched polyamidoamines for polymer flooding emulsions and microemulsions. Processes. **8**(2), 176 (2020)
42. Jiang, Z.Y., Yang, H., Xu, Y., et al.: A viscoelastic self-regulating agent for enhance oil recovery. Colloids Surf. A Physicochem. Eng. Asp. **603**, 125267 (2020)
43. Quan, H., Li, H., Huang, Z., et al.: Copolymer MCJS as a retarder of the acid-rock reaction speed for the stimulation of deep carbonate reservoirs. J. Appl. Polym. Sci. **132**(7), 41471 (2015)
44. Yang, B., Mao, J., Zhao, J., et al.: Improving the thermal stability of hydrophobic associative polymer aqueous solution using a "triple-protection" strategy. Polymers. **11**(6), 949 (2019)
45. Wang, Z.-Y., Lin, M.-Q., Li, H.-K., et al.: Plugging property and displacement characters of a novel high-temperature resistant polymer nanoparticle. Pet. Sci. **19**(1), 387–396 (2022)
46. Wang, Y., Liu, H., Wang, J., et al.: Formulation development and visualized investigation of temperature-resistant and salt-tolerant surfactant-polymer flooding to enhance oil recovery. J. Pet. Sci. Eng. **174**, 584–598 (2019)
47. Silva, I.P.G., Aguiar, A.A., Rezende, V.P. et al.: A polymer flooding mechanism for mature oil fields: laboratory measurements and field results interpretation. J. Pet. Sci. Eng. **161**, 468–475 (2018)
48. Sarsenbekuly, B., Kang, W. Fan, H., et al.: Study of salt tolerance and temperature resistance of a hydrophobically modified polyacrylamide based novel functional polymer for EOR. Colloids Surf a-Physicochem Eng. Aspects. **514**, 91–97 (2017)
49. Pu, W., Jiang, F., Wei, B., et al.: Influences of structure and multi-intermolecular forces on rheological and oil displacement properties of polymer solutions in the presence of Ca2+/Mg2+. RSC Adv. **7**(8), 4430–4436 (2017)
50. Jia, H., Chen, H.: The potential of using Cr3+/salt-tolerant polymer gel for well workover in low-temperature reservoir: laboratory investigation and pilot test. Spe. Prod. Oper. **33**(3), 569–582 (2018)
51. Hao, T., Zhong, L., Liu, J., et al.: Mechanistic study on the decrease in Injectivity during salt-resistant polymer flooding. ACS Omega. **7**(13), 11293–11304 (2022)